Atomic configuration, stabilizing mechanism, and impurity vibrations of carbon-oxygen complexes in crystalline silicon

C. Kaneta
Fujitsu Laboratories Ltd., 10-1 Morinosato-Wakamiya, Atsugi 243-01, Japan

T. Sasaki
National Research Institute for Metals, Meguro-ku, Tokyo 153, Japan

H. Katayama-Yoshida
Department of Physics, Tohoku University, Sendai 980, Japan
(Received 30 December 1991)

We have investigated the atomic configuration, stabilizing mechanism, and impurity vibrations of the carbon-oxygen complexes in silicon using norm-conserving pseudopotentials with the supercell method. We have found that a configuration in which an oxygen atom occupies a second-neighbor bond-interstitial site of a substitutional carbon atom without a direct C-O bond (CO-2 configuration) is more stable than the configuration in which an oxygen atom occupies a first-neighbor bond-interstitial site with a direct C-O bond (CO-1 configuration). The calculated total-energy reduction in the formation of the complex of the CO-2 configuration is 1.17 eV. Lattice-relaxation is essential to this stability. The previously observed infrared-absorption lines at 589, 640, 690, and 1104 cm^{-1} due to a C-O complex are well explained with the carbon- or oxygen-localized impurity vibrational modes calculated for the CO-2 configuration. Based on the comparison between the calculated and observed impurity vibrational energies, a type of configuration is suggested to explain another set of absorption lines at 716, 725, 744, and 1052 cm^{-1}.

I. INTRODUCTION

Oxygen and carbon are the most common impurities in Czochralski-grown silicon crystals. The interaction between them in silicon crystals has been the subject of much research for its technological importance, because precipitated oxygen acts as a gettering center for metallic impurities,[1] and because carbon enhances the oxygen precipitation.[2] Nevertheless, the nature of the interaction has not been well understood.

In an isolated configuration, oxygen in a silicon lattice stably occupies a bond-interstitial site, forming a slightly bent Si-O-Si bond,[3-10] and rotates almost freely around the original Si-Si bond ($\langle 111 \rangle$ axis).[11-13] Isolated carbon in silicon is usually a substitutional impurity.[14] Impurity vibrations of the isolated bond-interstitial oxygen (O_i) and the isolated substitutional carbon (C_s) cause infrared-absorption lines at 1136 and 607 cm^{-1}, respectively.[3,14]

Newman and Smith[15] and Bean and Newman[16] have studied as-grown Czochralski silicon crystals containing about 10^{18} cm^{-3} oxygen and various concentrations of carbon up to about 2×10^{18} cm^{-3}. They have found three satellite lines at 589, 640, and 690 cm^{-1} near the 607-cm^{-1} fundamental infrared-absorption line due to isolated C_s. They have also found a satellite line at 1104 cm^{-1}, near the 1136-cm^{-1} fundamental line due to isolated O_i. In crystals doped with ^{13}C or ^{14}C, they observed isotopic splitting for the 589-, 640-, and 690-cm^{-1} lines, but detected no splitting for the 1104-cm^{-1} line. From the isotopic splitting, the relative strength of the 589-, 640-, 690-, and 1104-cm^{-1} lines, and the dependence of the line strengths on carbon concentration, they attributed the lines to vibrations of the carbon-oxygen complex containing one carbon atom. (We refer to this as complex *A* in the following text.) They proposed that this complex contains one oxygen atom by analyzing the relations between the strengths of the lines, but this has not been confirmed. They have reported another C-O complex with a lower concentration, which was also attributed to a complex containing one carbon and one oxygen atom. (We refer to this as complex *B*.) This complex causes an oxygen-related infrared-absorption line at 1052 cm^{-1}, and carbon-related lines at 716, 724, and 744 cm^{-1}. The observed small shifts of the satellite lines of complex *A* from the C_s and O_i fundamental lines suggest that the atomic configurations around isolated C_s and O_i are almost retained in the C-O complex. Based on the lack of detectable ^{13}C and ^{14}C isotope splitting for the 1104- and 1052-cm^{-1} lines, Newman and Smith[15] proposed a model for the C-O complexes in which an oxygen atom occupies a second- or third-neighbor interstitial site of substitional carbon without a direct C-O bond. However, definitive atomic models for the complexes *A* and *B* have not yet been established. Shirakawa, Yamada-Kanata, and Ogawa also observed the two oxygen satellite lines at 1104 and 1052 cm^{-1}, and six other lines related to C-O complexes. They have found that complex *B* is less thermally stable than complex *A*.[17,18]

We have reported the stability of two types of C-O

complexes in silicon, in terms of total energy, using *ab initio* norm-conserving nonlocal pseudopotentials with the supercell method in local-density approximation.[19] In this paper, we present a more detailed study of our previous calculations, adding data on impurity vibrations, and propose atomic configurations for complexes *A* and *B*. In Sec. II, we briefly describe the model and method used in our calculation. In Sec. III, we show the results of our calculation for the stable atomic configuration, the stabilizing mechanism, and the oxygen- and carbon-localized impurity vibrations originating in the C-O complexes. We examine two types of atomic configurations as candidates for the C-O complexes, focusing on whether carbon and oxygen form a direct C-O bond in silicon crystal or not. A comparison between energies of the two configurations clarifies what kind of interaction dominates in stabilizing the C-O complex in silicon crystals. Calculated impurity vibrational energies of oxygen and carbon for the two types of C-O complexes are shown and compared with experimental data. The observed infrared-absorption lines of complex *A* are well explained by vibrational modes due to the C-O complex without a direct C-O bond. We also suggest an atomic configuration which explains complex *B* based on the comparison. Finally, in Sec. IV, we give a summary of our main results.

II. MODEL AND METHOD

Based on the experimental data by Newman and Smith[15] and Bean and Newman,[16] we assumed that the C-O complexes contain a substitutional carbon atom and a bond-interstitial oxygen atom. We examined two types of atomic configurations, CO-1 and CO-2. In the CO-1 configuration, an oxygen atom occupies one of the first-neighbor bond-interstitial sites of a substitutional carbon atom, with a direct C-O bond. In CO-2, the oxygen atom occupies one of the second-neighbor bond-interstitial sites without a direct C-O bond. Figure 1 shows the supercells used in our calculations. We used the supercells shown in Fig. 1(a) for isolated C_s and (b) for isolated O_i, as reference systems for the comparison in Sec. III. The supercells for CO-1 and CO-2 are shown in Figs. 1(c) and 1(d). They contain one oxygen, one carbon, and seven silicon atoms.

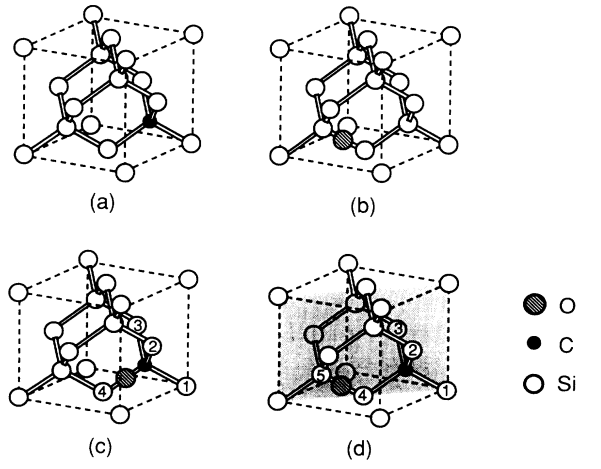

FIG. 1. Supercells used for (a) isolated C_s, (b) isolated O_i, (c) CO-1, and (d) CO-2 configurations. The shadowed (110) plane in (d) is a mirror plane.

The stable Si-O-Si and Si-O-C structures in the isolated O_i, CO-2, and CO-1 configurations are slightly bent in our preliminary calculation.[20] Needels *et al.*[21] also obtained such a bent structure for Si-O-Si using almost the same calculation method as ours. In the present calculation, however, we restricted the structures of Si-O-Si and Si-O-C to be linear, i.e., we restricted the symmetry of the stable CO-1, CO-2, and isolated O_i configurations to C_{3v}, C_{1h}, and D_{3d}, respectively. Our choice of such linear structures is based on the following results of previous work. In the case of isolated O_i, the stable Si-O-Si structure is nearly linear.[3-10] The energy difference between the stable bent and the linear Si-O-Si structures is estimated to be less than 50 meV.[10-13] The above-mentioned restriction, therefore, would not so much affect the calculational results of the total energy and the atomic configuration, apart from the off-axis relaxation of O_i from the Si-Si ($\langle 111 \rangle$) axis, if any. Moreover, this choice of the straight Si-O-Si structure leads to an unambiguous model to describe oxygen's vibration. The adiabatic potential for oxygen's off-axis displacement is well approximated by an axially symmetric potential with a low-energy barrier at the on-axis site.[10-13] Because the barrier is low enough, the bent bridged Si-O-Si structure easily changes to the oppositely bent configuration by axis-perpendicular motion of the oxygen. Therefore, the bent bridged Si-O-Si structure, which might be stable is the statical point of view, is not physically meaningful as a starting point to discuss the oxygen vibrations. By employing the straight Si-O-Si structure as the origin of the atomic displacements, we can separate oxygen's axis-parallel and axis-perpendicular motions. This is an unambiguous zeroth-order approximate description of the vibration, which is good enough for our present purpose. We checked the difference between the vibrational energies calculated with the straight and the bent bridged Si-O-Si structures by the linear combination of atomic orbitals (LCAO) method.[10] We obtained 10% for the experimentally observed 1136-cm^{-1} mode, and 1% for another infrared-active mode observed at 517 cm^{-1}. For the C_s-O_i complexes, this argument would be also valid because the relatively small shifts of the 1104- and 1052-cm^{-1} lines from the isolated oxygen line at 1136 cm^{-1} suggest that the change in the atomic configuration of O_i caused by carbon is not so large. Actually, our preliminary calculation[20] suggests that the stable Si-O-Si and Si-O-C structures in the CO-1 and CO-2 configurations, respectively, are also nearly linear and that the energy differences between the stable bent and the linear structures are small. The effect of the restriction on the Si-O-Si or Si-C-O structures only appears in the missing of energy splitting of the carbon mode in the CO-1 configuration, which will again be mentioned in Sec. III B. For the stable configuration of isolated C_s, the symmetry is restricted to T_d. Restricting the symmetries of the systems as mentioned above reduces the amount of calculations.

The total energy for each configuration was calculated using the norm-conserving nonlocal pseudopotentials tabulated by Bachelet, Hamann, and Schluter.[22] The Ceperley-Alder form parametrized by Perdew and Zunger[23,24] was used for the exchange-correlation energy. The stable atomic positions of oxygen, carbon, and their neighboring silicon atoms in each configuration were determined by calculating the Hellmann-Feynman force[25] with the above-mentioned restrictions on symmetry. To compare the total energy of each system, equivalent sets of special points in the Brillouin zone containing 4, 10, 10, and 20 **k** points were used according to the symmetry of isolated C_s, isolated O_i, CO-1, and CO-2 configurations, respectively. The energy cutoff of the plane-wave basis was set at 29.16 Ry. We checked the dependence of the calculated results on the energy cutoff from 16 to 29.16 Ry, and confirmed that this cutoff energy is enough for our purpose, although a larger cutoff energy is needed for the total energy of a system containing oxygen to converge.[26]

In this framework, the calculated lattice constant of a perfect silicon crystal is 5.37 Å, well reproducing the experimental value, 5.43 Å, the error being only about 1%. In our calculations, we fix the lattice constant to this calculated value.

III. RESULTS

A. Stable atomic configuration and the stabilizing mechanism

The calculated stable atomic positions and valence-charge-density distributions of CO-1 and CO-2 projected onto the (110) plane are shown in Figs. 2(a) and 2(b), respectively. The bond lengths and bond angles around carbon and oxygen for the calculated stable isolated O_i, isolated C_s, CO-1, and CO-2 configurations are listed in Table I. The deviations of the stable atomic positions calculated at 29.16 Ry from the converged positions are estimated by extrapolating the calculated positions with respect to the cutoff energy. The extrapolation gives 0.03 Å for carbon in CO-1, 0.02 Å for silicon located between carbon and oxygen in CO-2, and less than 0.01 Å for all other atoms. The order of the calculated bond lengths listed in Table I, therefore, does not change, even if we extend the cutoff energy. The calculated Si-O bond lengths in CO-1 (1.65 Å) and CO-2 (1.64 Å) are slightly larger than calculated for isolated O_i (1.62 Å), due to the lattice relaxation caused by carbon. In the CO-2 configuration, the calculated values of the two Si-O bond lengths are the same, even though we put no restrictions on them. On the other hand, the C-Si bond lengths in CO-1 and CO-2 are smaller than the length of 2.14 Å calculated for isolated C_s. The C-O bond length (1.42 Å) is much smaller than O-Si and C-Si bond lengths, corresponding to a strong bond between carbon and oxygen. In the CO-2 configuration, we find a large displacement of the silicon atom located between carbon and oxygen, 0.56 Å, from its original position in the perfect silicon crystal.

The change of total energy in the formation of the C-O complex in silicon is calculated from

$$\Delta E_{\mathrm{CO}}=(E_{\mathrm{CO}}+E_{\mathrm{Si}})-(E_{\mathrm{C}_s}+E_{\mathrm{O}_i}) , \tag{1}$$

where E_{CO}, E_{C_s}, and E_{O_i} are the total energies of systems containing the C-O complex in the CO-1 or CO-2 configuration, isolated C_s, and isolated O_i. E_{Si} is the total energy of the pure silicon system. The convergence of ΔE_{CO} for CO-1 and CO-2 as a function of plane-wave cutoff energy was tested from 16 to 29.16 Ry (Fig. 3). For the CO-1 configuration, ΔE_{CO} has not yet converged. For the CO-2 configuration, ΔE_{CO} converges to -1.17 eV. The CO-2 configuration is therefore stable as a C-O complex. At this stage, the stability of the CO-1 configuration as a C-O complex is not conclusive. However, it is at least clear that the CO-1 configuration is not as stable as the CO-2 configuration.

To understand the stabilizing mechanism of the C-O complex, we separate the total energy of a system into two parts, the *electrostatic* and *electronic* parts. Here, we define the electrostatic energy of a system by

$$E_s=E_{ii}-E_{ie}+E_{ee} , \tag{2}$$

where

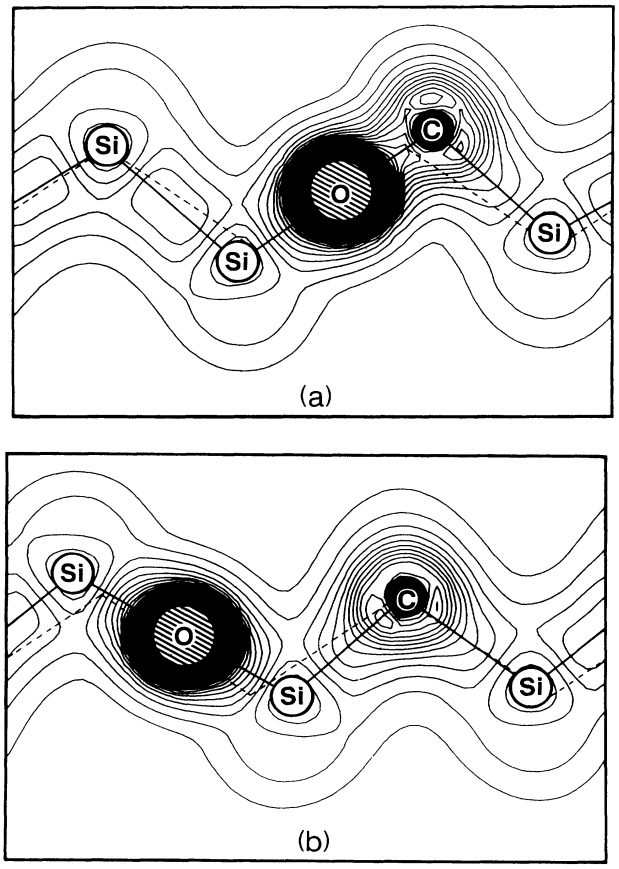

FIG. 2. Calculated stable atomic positions and the valence-charge-density distributions in the (110) plane for (a) CO-1 and (b) CO-2 configurations. The dashed lines show the original bond structure in the perfect silicon crystal.

TABLE I. Calculated bond lengths and bond angles for optimized atomic positions in isolated O_i, isolated C_s, CO-1, and CO-2 configurations. All lengths are in Å and all angles are in degrees. The number given to each silicon atom corresponds to the number in Fig. 1.

Configuration	Symmetry	Bond	Bond length (bond angle)
Isolated O_i	D_{3d}	O-Si	1.62
Isolated C_s	T_d	C-Si	2.14
		Si-C-Si	(109.47)
CO-1	C_{3v}	O-Si(4)	1.65
		C-Si(1)	2.05
		C-O	1.42
		O-C-Si(1)	(100.92)
		Si(1)-C-Si(2)	(116.49)
CO-2	C_{1h}	O-Si(4)	1.64
		O-Si(5)	1.64
		C-Si(1)	2.01
		C-Si(2)	2.12
		C-Si(4)	1.96
		Si(1)-C-Si(2)	(113.41)
		Si(1)-C-Si(4)	(99.24)
		Si(2)-C-Si(3)	(105.15)
		Si(2)-C-Si(4)	(112.94)

$$E_{ii}=\frac{1}{2}\sum_{\substack{\mu,\nu\\ \mu\neq\nu}}\frac{2Z_\mu Z_\nu}{|\mathbf{R}_\mu-\mathbf{R}_\nu|}\ , \tag{3}$$

$$E_{ie}=\sum_\mu\int\frac{2Z_\mu}{|\mathbf{r}-\mathbf{R}_\mu|}\rho_0 d\mathbf{r}\ , \tag{4}$$

$$E_{ee}=\frac{1}{2}\int\int\frac{2}{|\mathbf{r}-\mathbf{r}'|}\rho_0^2 d\mathbf{r}\,d\mathbf{r}'\ . \tag{5}$$

Rydberg units are used in this equation. Z_μ is the valence of the μth ion core and the $\mathbf{R}_\mu$ is the position vector of the μth atom. ρ_0 is the average density of valence electrons in the system. E_s depends only on the configuration of the ion cores and is independent of the valence-charge distribution. The electronic energy E_e is defined by

$$E_e=E_t-E_s\ , \tag{6}$$

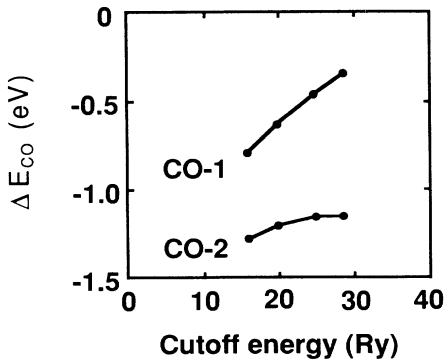

FIG. 3. Convergence of the total energy change, ΔE_{CO}, for CO-1 and CO-2 as a function of plane-wave cutoff energy.

TABLE II. Electrostatic and electronic parts of calculated ΔE_{CO} in eV. The cutoff energy is fixed at 29.16 Ry. Each part of the energy calculated for the configuration containing isolated O_i and isolated C_s together is taken to be zero.

	CO-1	CO-2
Electronic	−33.72	2.92
Electrostatic	33.36	−4.09
Total	−0.36	−1.17

where E_t is the total energy of a system. Table II compares the electrostatic and electronic parts of the change of total energy ΔE_{CO} in the CO-1 and CO-2 configurations. The electronic part of ΔE_{CO} decreases when carbon and oxygen approach each other to take the CO-1 configuration, strongly hybridizing carbon sp^3 and oxygen $2p$ orbitals, and producing the large buildup of valence charge between carbon and oxygen shown in Fig. 2(a). At the same time, the electrostatic part, which is related to lattice relaxation, increases. As a result, the total energy does not decrease largely in this configuration. In CO-2, the decrease in the electrostatic part of ΔE_{CO} lowers the total energy, making this configuration more stable than CO-1. We checked the dependence of this result on the cutoff energy. For CO-1, as the cutoff energy increases, with the stable C-O bond length decreasing, the electrostatic part of ΔE_{CO} continues to increase and the electronic part continues to decrease. In contrast, the two parts of ΔE_{CO} in CO-2 are unchanged for cutoff energies over 25 Ry. The above-mentioned result is not therefore changed even for the infinity limit of the cutoff energy.

To confirm this stabilizing mechanism, we carried out a calculation without lattice relaxation. In the calculation for E_{CO}, E_{O_i}, and E_{C_s}, we replaced one of the silicon atoms with a carbon atom and placed an oxygen atom at a bond-center site. Displacement of the silicon atoms around the incorporated impurity atoms was not allowed. The result is shown in Table III. We find that CO-1 is more stable than CO-2 when lattice relaxation is inhibited. The lattice relation therefore plays an essential role to determine the stability of the C-O complex.

B. Impurity vibrations

For the optimum atomic configurations obtained above, we calculated the impurity vibrational energies of oxygen and carbon. Prior to the calculation for the C-O complexes, we roughly checked the cutoff energy dependence of vibrational energies for isolated C_s and isolated O_i. The calculated energies increase as the cutoff energy

TABLE III. Electrostatic and electronic parts of ΔE_{CO} calculated without lattice relaxation. All energies are in eV.

	CO-1	CO-2
Electronic	−1.10	−0.12
Electrostatic	0	0
Total	−1.10	−0.12

increases. The vibrational energies of isolated C_s and isolated O_i calculated at 29.16 Ry, at which the cutoff energy is fixed in the following calculation, are 2% and 5% larger, respectively, than the vibrational energies calculated at 20.25 Ry.

The vibrational energies of oxygen-localized antisymmetric stretching modes of Si-O-Si in CO-2 and in isolated O_i, and Si-O-C in CO-1 were calculated taking account of the coupling between the motion of oxygen and of the adjacent silicon or carbon atoms. Table IV lists the results and compares them with the experimental results. The calculated energy for isolated O_i, 1221 cm^{-1}, is 7.4% larger than the experimental value, 1136 cm^{-1}. This is mainly because of the small supercell size we used. We therefore only discuss the trend of the shifts of the vibrational energies from that of the isolated O_i. The calculated value for CO-2, 1154 cm^{-1}, is lower than for isolated O_i, consistent with the fact that the observed oxygen lines of complexes *A* and *B* are on the lower-energy side of the isolated O_i line. The stretching force constants calculated for the Si-O bonds in CO-2 and isolated O_i configurations are 4.9×10^5 and 5.5×10^5 dyn/cm, respectively. Almost the same values, 4.9×10^5 and 5.07×10^5 dyn/cm, have been obtained for the Si-O bond length in isolated O_i,[8] and for vitreous SiO_2,[27] respectively. In the CO-2 configuration, the slight increase in the Si-O bond length, caused by the relaxation of the silicon atom between carbon and oxygen, causes the reduction in the force constant and, as a result, the reduction in the vibrational energy of oxygen. The calculated value for CO-1, 1253 cm^{-1}, is higher than that for isolated O_i, and contradicts the fact that the observed oxygen lines caused by complexes *A* and *B* are on the lower-energy side of the line due to isolated O_i. This is explained by the large stretching force constant of the C-O bond, 8.5×10^5 dyn/cm, which is 1.8 times larger than the stretching force constant of the Si-O bond in CO-1, 4.7×10^5 dyn/cm. This result suggests that the atomic configurations of both complex *A* and complex *B* are not of the CO-1 type with a direct C-O bond.

TABLE IV. Impurity vibrational energies of oxygen and carbon in isolated O_i, isolated C_s, CO-1, and CO-2 configurations. The cutoff energy is fixed at 29.16 Ry. All energies are expressed in wave number (cm^{-1}). The ratio of the shifts of the vibrational energies of oxygen and carbon in complexes from those of isolated O_i or C_s are shown in % in parenthesis. Experimental data are taken from the Refs. 3 and 14–16.

Configuration	Origin	Calculation	Experiment
Isolated O_i	O	1221	1136
Isolated C_s	C	450	607
CO-2, Complex *A*	O	1154 (−5.4)	1104 (−2.8)
	C	395 (−12.2)	589 (−2.9)
	C	509 (13.1)	640 (5.4)
	C	543 (20.6)	690 (13.6)
CO-1	O	1253 (2.6)	
	C	713 (58.4)	
	C	413 (−8.2)	
Complex *B*	O		1052 (−7.4)
	C		716 (18.0)
	C		724 (19.3)
	C		744 (22.6)

Table IV also lists the results for carbon-localized modes and compares them with experimental data. The coupling between the motion of the carbon and those of surrounding atoms is neglected in this calculation. If we take the coupling into account in the case of isolated C_s, we obtain the vibrational energy, 471 cm^{-1}, which is 4.6% larger than the value of 450 cm^{-1} obtained when we neglect the coupling. Again, because of the small supercell size we used, incomplete lattice relaxation may cause residual tension around a carbon atom and lower the vibrational energy. We therefore only discuss the trend of the shifts of the vibrational energies from that of the isolated C_s.

In the CO-1 configuration, whose symmetry is C_{3v}, the triply degenerate T_2 vibrational mode of isolated C_s splits into two modes, *E* and A_1. In the doubly degenerate *E* mode, the direction of motion of the carbon atom is in the plane perpendicular to the C-O bond. The calculated vibrational energy of this mode is 413 cm^{-1}, which is lower than that of isolated C_s, 450 cm^{-1}. This softening is due to the strong electrostatic repulsion between carbon and oxygen arising from the electrostatic part of the total energy E_s in Eq. (2). This repulsion reduces the stability of the carbon atom with respect to its displacement perpendicular to the C-O bond. If we account for the small bending of the Si-O-C bond neglected here, and if the rotation of oxygen around the ⟨111⟩ axis is quenched, the *E* mode splits slightly. The A_1 mode is a totally symmetric C-O bond stretching mode. The vibrational energy calculated for this mode is 713 cm^{-1}, 58% larger than the 450 cm^{-1} obtained for isolated C_s. This is because of the strong C-O bond. This energy shift of the A_1 mode caused by the formation of the complex is very large compared to any carbon line shift observed for complex *A* and *B* (see Table IV). This also excludes the possibility of the CO-1 configuration as a candidate for complex *A* or *B*.

In the CO-2 configuration, C, Si(4), and O are on a mirror plane, as shown in Fig. 1(d). The symmetry of this configuration is C_{1h}. Three nondegenerate carbon-localized modes appear for this configuration. Two of them are the totally symmetric *A* modes in which the carbon atom displaces in the mirror plane. The vibrational energies calculated for these modes are 509 and 543 cm^{-1}, which are higher than that calculated for the original T_2 mode of isolated C_s. This is because oxygen causes compressive stress at the carbon site in the mirror plane. In the other mode, the *B* mode, the carbon atom displaces perpendicular to the mirror plane. The calculated vibrational energy for this mode is 395 cm^{-1}, which is lower than that for the T_2 mode of isolated C_s.

Consequently, the impurity vibrations observed for complex *A* are well explained by the results for CO-2. For complex *B*, however, all energies of the carbon satellites are higher than that of the fundamental line, 607

cm^{-1}, meaning that the configuration of complex *B* cannot be CO-2 or CO-1.

IV. DISCUSSION

Here we discuss the atomic configurations of complexes *A* and *B*, based on the comparison between the calculated and observed impurity vibrational energies. We find that all energy shifts of O_i and C_s lines of complex *A* from their fundamental lines are well explained by the CO-2 configuration. We therefore assign complex *A* to the CO-2 configuration.

In this calculation, we examined only the CO-1 and CO-2 configurations. But, based on the calculations presented above, it is suggested that, if CO-*N* ($N \geq 3$) configuration in which oxygen occupies an *N*th-neighbor bond-interstitial site of a carbon atom is stable as a C-O complex, the stabilizing mechanism would be the same as for the CO-2 configuration, because carbon and oxygen do not have a direct C-O bond in the configuration. For example, in the CO-4 configuration in Fig. 4, whose symmetry is also C_{1h}, the trend of the vibrational energy shifts of carbon and oxygen would be qualitatively the same as in the CO-2 configuration. The shifts in vibrational energy would be smaller than those in the CO-2 configuration because, in the CO-4 configuration, the change of the atomic configuration around carbon and oxygen in the formation of the complex is smaller than in the CO-2 configuration. Based on this consideration, the possibility that complex *A* is assigned to CO-4 configuration, therefore, remains.

Next, we discuss candidates for complex *B*. The absorption lines of complex *B* are not explained by the CO-1 or CO-2 configuration. All of the observed carbon satellites of complex *B* are on the higher-energy side of the isolated C_s line. The large energy shift of the carbon satellites to higher energies and the small splitting between them suggest that compressive stress around the carbon atom in complex *B* is large and isotropic. This is not explained by anisotropic configurations such as CO-1, CO-2, or CO-4. At least one more oxygen atom, for example outside the mirror plane in Fig. 1(d), may be needed to explain the absorption lines at 716, 724, and 744 cm^{-1} of complex *B*. In this point, our model for complex *B* is different from that proposed by Bean and Newman,[16] which contains only one oxygen atom.

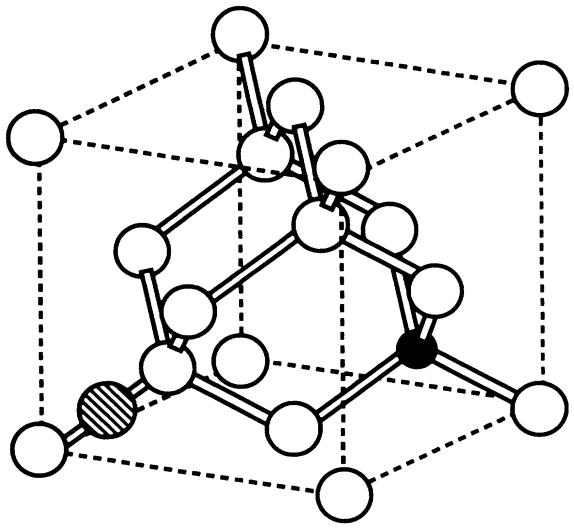

FIG. 4. Atomic configuration of CO-4. The symbols for carbon, oxygen, and silicon are the same as in Fig. 1.

We have shown that the CO-2 configuration is stable for a C-O complex. Configurations like CO-2, without a direct C-O bond, would be convenient for several oxygen atoms to gather around a carbon atom. Oxygen at one of the second-neighbor interstitial sites of carbon would not largely disturb the network of silicon around the carbon atom, because the displacement of carbon from the ideal substitutional site is small in the CO-2 configuration. When the next oxygen atom approaches a C-O complex, it could occupy an interstitial site near the carbon atom. In this way, at least a few oxygen atoms may aggregate around a carbon atom.

V. CONCLUDING REMARKS

We have investigated the stable atomic configuration, stabilizing mechanism, and impurity vibrations of C-O complexes in silicon using norm-conserving pseudopotentials with the supercell method. We have found that a substitutional carbon atom and an interstitial oxygen atom form a stable C-O complex. The CO-2 configuration, in which an oxygen atom occupies a second-neighbor bond-interstitial site of a carbon atom without a direct C-O bond, is stable for a C-O complex. The calculated total-energy reduction in the formation of isolated C_s and O_i into a complex of the CO-2 configuration is 1.17 eV. We could not determine the stability of the CO-1 configuration with a direct C-O bond. But, at least, it is not as stable as the CO-2 configuration. We compared the calculational results with and without lattice relaxation around the impurities and have found that lattice relaxation is essential to the stability of C-O complexes. We have also calculated the vibrational energies of oxygen and carbon in the CO-1, CO-2, isolated C_s, and isolated O_i configurations. The CO-1 configuration does not explain the absorption lines observed for either complex *A* or *B*, meaning that neither complex *A* nor *B* has this configuration. The results for the CO-2 configuration well explain the set of infrared absorption lines at 589, 640, 690, and 1104 cm^{-1} observed by Newman *et al.* In the CO-2 configuration, oxygen causes compressive stress around carbon mainly in the $\langle 110 \rangle$ plane which contains carbon, oxygen, and silicon located between them. We have assigned the carbon-related absorption line at 589 cm^{-1} to carbon vibration perpendicular to the $\langle 110 \rangle$ plane, and the lines at 640 and 690 cm^{-1} to vibrations in the plane. To explain another set of lines at 716, 724, 744, and 1052 cm^{-1}, it may be necessary to consider at least two oxygen atoms in a complex.

ACKNOWLEDGMENTS

One of the authors (C.K.) is grateful to H. Yamada-Kaneta and Y. Shirakawa for helpful discussion and for providing their experimental data before publication. She is also grateful to Dr. A. Ohsawa, N. Nakayama, and Dr. T. Ito for their support.

[1]T. Y. Tan, E. E. Gardner, and W. K. Tice, Appl. Phys. Lett. **30**, 175 (1977).
[2]R. A. Craven, in *Semiconductor Silicon,* edited by H. R. Huff, R. J. Krieger, and Y. Takeishi (Electrochemical Society, Pennington, NJ, 1981), p. 254.
[3]W. Kaiser, P. H. Keck, and C. F. Lange, Phys. Rev. **101**, 1264 (1956).
[4]H. J. Hrostowski and R. H. Kaiser, Phys. Rev. **107**, 966 (1957).
[5]W. L. Bond and W. Kaiser, J. Phys. Chem. Solids **16**, 44 (1960).
[6]J. W. Corbett, R. S. McDonald, and G. D. Watkins, J. Phys. Chem. Solids **25**, 873 (1964).
[7]M. Saito and A. Oshiyama, Phys. Rev. B **38**, 10 711 (1988).
[8]E. Martinez, J. Plans, and F. Yndurain, Phys. Rev. B **36**, 8043 (1987).
[9]L. C. Snyder and J. W. Corbett, in *Proceedings of the 13th International Conference on Defects in Semiconductors,* edited by L. C. Kimerling and J. M. Parsey, Jr. (Metallurgical Society of AIME, New York, 1985), p. 693.
[10]C. Kaneta, H. Yamada-Kaneta, and A. Ohsawa, in *Proceedings of the 15th International Conference on Defects in Semiconductors,* edited by G. Ferenczi, Vols. 38–41 of Materials Science Forum (Trans Tech, Aedermannsdorf, 1989), p. 323.
[11]D. R. Bosomworth, W. Hayes, A. R. L. Spray, and G. D. Watkins, Proc. R. Soc. London Ser. A **317**, 133 (1970).
[12]H. Yamada-Kaneta, C. Kaneta, T. Ogawa, and K. Wada, in *Proceedings of the 15th International Conference on Defects in Semiconductors* (Ref. 10), p. 637.
[13]H. Yamada-Kaneta, C. Kaneta, and T. Ogawa, Phys. Rev. B **42**, 9650 (1990).
[14]R. C. Newman and J. B. Willis, J. Phys. Chem. Solids **26**, 373 (1965).
[15]R. C. Newman and R. S. Smith, J. Phys. Chem. Solids **30**, 1493 (1969).
[16]A. R. Bean and R. C. Newman, J. Phys. Chem. Solids **33**, 255 (1972).
[17]Y. Shirakawa, H. Yamada-Kanata, and T. Ogawa, in *Proceedings of the Symposium on Advanced Science and Technology of Silicon Materials* (Japan Society for the Promotion of Science, The 145th Committee, Tokyo, 1992), p. 56.
[18]Y. Shirakawa, H. Yamada-Kanata, and T. Ogawa, in *Proceedings of the 5th International Conference on Shallow Impurities in Semiconductors* (Trans Tech, Aedermannsdorf, in press).
[19]C. Kaneta, H. Katayama-Yoshida, and T. Sasaki, in *Proceedings of the 20th International Conference on the Physics of Semiconductors,* edited by E. M. Anastassakis and J. D. Joannopoulos (World Scientific, Singapore, 1990),Vol. 1, p. 561.
[20]C. Kaneta (unpublished).
[21]M. Needels, J. P. Joannopoulos, Y. Bar-Yam, and S. T. Pantelides, Phys. Rev. B **43**, 4208 (1991).
[22]G. B. Bachelet, D. R. Hamann, and M. Schluter, Phys. Rev. B **26**, 4199 (1982).
[23]D. M. Ceperley and B. J. Alder, Phys. Rev. Lett. **45**, 566 (1980).
[24]J. P. Perdew and A. Zunger, Phys. Rev. B **23**, 5048 (1981).
[25]J. Ihn, A. Zunger, and M. L. Cohen, J. Phys. C **12**, 4401 (1979).
[26]Y. Bar-Yam, S. T. Pantelides, and J. P. Joannopoulos, Phys. Rev. B **39**, 3396 (1989).
[27]R. A. Barrio, F. L. Galeener, and E. Martinez, Phys. Rev. B **31**, 7779 (1985).

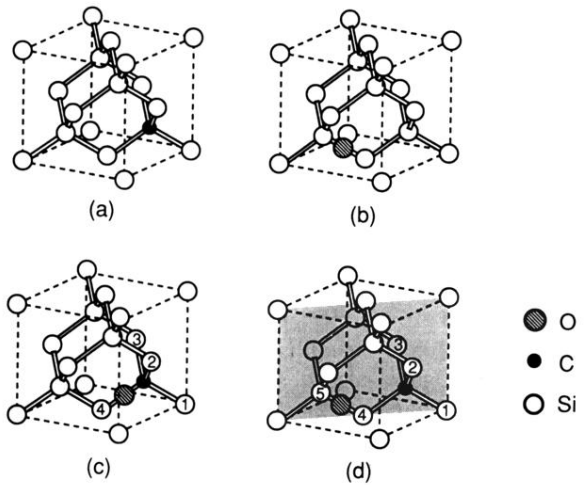

FIG. 1. Supercells used for (a) isolated C_s, (b) isolated O_i, (c) CO-1, and (d) CO-2 configurations. The shadowed (110) plane in (d) is a mirror plane.